

Dynamics of a Cr spin in a semiconductor quantum dot: Hole-Cr flip-flops and spin-phonon coupling

A. Lafuente-Sampietro,^{1,2} H. Utsumi,² M. Sunaga,² K. Makita,² H. Boukari,¹ S. Kuroda,² and L. Besombes^{1,*}

¹*Univ. Grenoble Alpes, CNRS, Grenoble INP, Institut Néel, 38000 Grenoble, France*

²*Institute of Materials Science, University of Tsukuba, 1-1-1 Tennoudai, Tsukuba 305-8573, Japan*



(Received 12 February 2018; published 2 April 2018)

A detailed analysis of the photoluminescence (PL) intensity distribution in singly Cr-doped CdTe/ZnTe quantum dots (QDs) is performed. First of all, we demonstrate that hole-Cr flip-flops induced by an interplay of the hole-Cr exchange interaction and the coupling with acoustic phonons are the main source of spin relaxation within the exciton-Cr complex. This spin flip mechanism appears in the excitation power dependence of the PL of the exciton as well as in the intensity distribution of the resonant PL. The resonant optical pumping of the Cr spin which was recently demonstrated can also be explained by these hole-Cr flip-flops. Despite the fast exciton-Cr spin dynamics, an analysis of the PL intensity under magnetic field shows that the hole-Cr exchange interaction in CdTe/ZnTe QDs is antiferromagnetic. In addition to the Cr spin dynamics induced by the interaction with carriers' spin, we finally demonstrate using time resolved optical pumping measurements that a Cr spin interacts with nonequilibrium acoustic phonons generated during the optical excitation inside or near the QD.

DOI: [10.1103/PhysRevB.97.155301](https://doi.org/10.1103/PhysRevB.97.155301)

I. INTRODUCTION

Individual spins in semiconductors are promising for the development of quantum technologies based on solid state devices. Important progress have been made recently for spins of carriers confined in nanostructures [1] and for electronic and nuclear spins localized on individual defects [2]. Diluted magnetic semiconductor systems combining high quality nanostructures and the properties of localized spins on transition metal elements are alternative good candidates for the development of such single spin quantum devices. Optically active quantum dots (QDs) containing individual or pairs of magnetic dopants can be realized both in II-VI [3–7] and III-V [8,9] semiconductors. In these systems, since the confined carriers and magnetic atom spins become strongly mixed, an optical excitation of the QD can affect the spin state of the atom offering possibilities for a probing and a control of the localized spin [10,11].

The variety of $3d$ transition metal magnetic elements that can be incorporated in conventional semiconductors gives a large choice of localized electronic and nuclear spins as well as orbital momentum [3,12–14]. For a given semiconductor nanostructure, the spin properties resulting from the exchange interaction between the confined carriers and the incorporated magnetic dopant strongly depend on the filling of the $3d$ orbital of the atom. The choice of a particular magnetic element can then be adapted for a targeted application. This approach opens a diversity of possible use of individual spins in diluted magnetic semiconductor nanostructures for quantum information technologies or quantum sensing.

Among these magnetic atoms, chromium (Cr) is of particular interest [14]. It incorporates in II-VI semiconductors

as Cr^{2+} carrying an electronic spin $S = 2$ and an orbital momentum $L = 2$. Moreover, most Cr isotopes have no nuclear spin. This simplifies the spin level structure and the coherent dynamics of its electronic spin [15]. With bi-axial strain, the ground state of the Cr is expected to be an orbital singlet with a spin degeneracy of 5. The Cr feature both spin and orbital degrees of freedom and the orbital momentum of the Cr atom connects its spin to the local strain through the modification of the crystal field and the spin-orbit coupling. This spin to strain coupling is more than two orders of magnitude larger than for elements without orbital momentum (NV centers in diamond [16], Mn atoms in II-VI semiconductors [17]).

In analogy with the spin structure of NV centers in diamond, the spin states $S_z = \pm 1$ of a Cr in a QD form a spin *qubit* coupled to in-plane strain [18]. The Cr spin is therefore a promising system for the realization of hybrid spin-mechanical devices in which the motion of a mechanical oscillator would be coherently coupled to the spin state of a single atom and probed or coherently controlled through this interaction [16,19,20].

The optical probing and some optical control of the spin of an individual Cr atom incorporated in a CdTe/ZnTe QD such as resonant optical pumping and optical Stark effect, were recently demonstrated [14,21]. In these first reports the excitation power dependence and the magnetic field dependence of the intensity distribution in the photoluminescence (PL) of the exciton in Cr-doped QDs as well as the mechanism of resonant optical pumping of the Cr spin were not analyzed. The PL intensity distribution and the pumping mechanism are a consequence of the spin dynamics of the Cr alone in the empty QD and of the dynamics of coupled carriers and Cr spins when the QD contains an exciton. The spin dynamics of highly diluted magnetic atoms in a semiconductor host is controlled by (i) the spin-spin coupling with carriers and (ii) the interaction with acoustic phonons (spin lattice coupling) [22]. We discuss

*lucien.besombes@neel.cnrs.fr

in this paper how these two spin relaxation mechanisms affect the optical properties of singly Cr-doped CdTe QDs.

After a short presentation of the samples and experiments in Sec. II we describe in Sec. III the excitation power dependence of the exciton-Cr PL intensity. It presents a nonintuitive behavior with an increase of the ratio of the PL intensities of the central and outer lines at high excitation power. We interpret this evolution as resulting from a transfer towards the Cr spin state $S_z = 0$ which is enhanced by the presence of the exciton in the QD. Time resolved resonant PL in the regime of optical pumping directly evidence efficient transfer from $S_z = \pm 1$ to $S_z = 0$. As a result, the exciton PL intensity cannot be simply considered as a probe of the spin state of the Cr atom. Despite this fast exciton-Cr spin dynamics which perturbs the Cr spin before the exciton recombination, the PL intensity distribution under magnetic field presented in Sec. IV shows that the hole-Cr exchange interaction in CdTe/ZnTe QDs is antiferromagnetic. With this antiferromagnetic interaction, we propose in Sec. V a mechanism which explains the observed transfer towards $S_z = 0$ and the resonant optical pumping of the Cr spin. It is based on hole-Cr flip-flops induced by an interplay of the hole-Cr exchange interaction and the coupling with the strain field of acoustic phonons. Finally in Sec. VI, using a spatially resolved two wavelength pump-probe experiment, we demonstrate that the dynamics of the Cr spin is also strongly affected by nonequilibrium phonons generated during the optical excitation.

II. SAMPLES AND EXPERIMENTS

To optically access an individual magnetic atom, Cr are randomly introduced in CdTe/ZnTe self-assembled QDs during their MBE growth [14,23]. A low density of Cr is chosen to allow for the detection of QDs containing zero, one or a few Cr atoms. The PL of individual QDs is studied by optical microspectroscopy at low temperature ($T = 5$ K). The PL is excited with a continuous wave (cw) dye laser tuned to an excited state of the QD, dispersed and filtered by a 1 m double spectrometer before being detected by a Si cooled multichannel charged coupled device (CCD) camera or a fast Si avalanche photodiode with a time resolution of about 350 ps. A magnetic field can be applied along the QD growth axis. A single-mode dye ring laser can also be tuned on resonance with the ground state of the exciton to perform time resolved resonant optical pumping experiments. In such experiments, trains of resonant and nonresonant light pulses with variable durations and wavelengths are generated from the cw lasers using acousto-optical modulators with a switching time of about 15 ns. The relative position of the sub- μm pump and probe laser spots can also be precisely controlled within a 10 μm range.

The PL spectra of an exciton in a Cr-doped QD (X-Cr) is reported in Fig. 1(a). Because of the large magnetic anisotropy of the Cr spin induced by the bi-axial strain in the plane of self-assembled QDs, the Cr spin thermalizes on the lowest energy states $S_z = 0$ and $S_z = \pm 1$. The magnetic anisotropy can be described by a spin effective Hamiltonian $D_0 S_z^2$ where z is the QD growth axis. This parabolic splitting shifts the $S_z = \pm 2$ spin states to high energy and no contribution of these

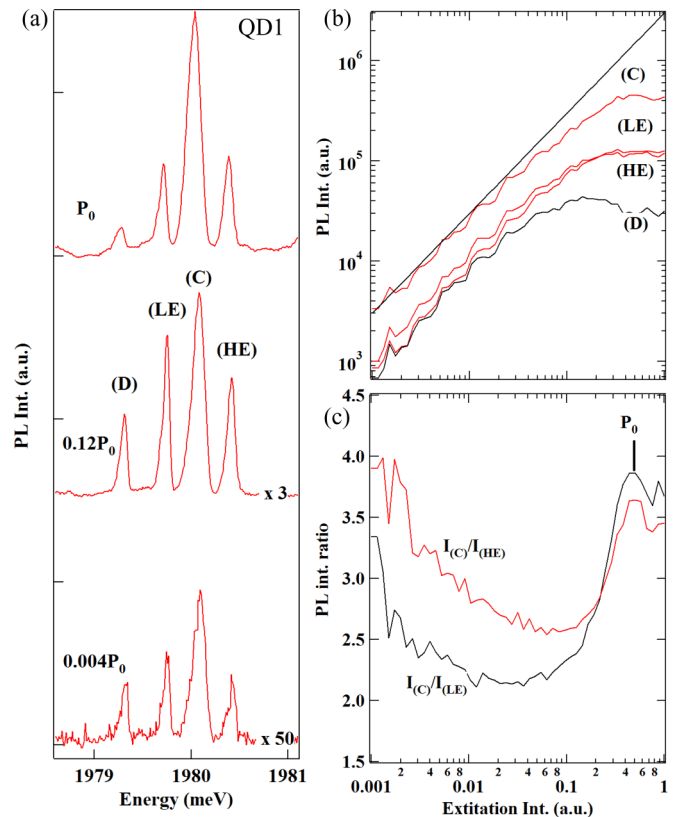


FIG. 1. (a) PL of the exciton in a Cr-doped QD (QD1) for three different excitation powers at $T = 5$ K. (b) Excitation power dependence of the PL intensities of the different exciton-Cr lines. The solid line is a linear fit. (c) Excitation power dependence of the PL intensity ratios of the central and low energy lines (I_C/I_{LE}) and central and high energy lines (I_C/I_{HE}).

states is observed in the PL in the investigated temperature range.

The exchange interaction with the spin of the bright excitons ($|\downarrow_h \uparrow_e\rangle$ or $|\uparrow_h \downarrow_e\rangle$) further splits the Cr states $S_z = \pm 1$ [14]. The PL of a Cr-doped QD is then dominated by three emissions lines, the two outer lines associated with the Cr spin states $S_z = \pm 1$ [labeled (LE) and (HE)] and the central line corresponding to $S_z = 0$ [labeled (C)]. Most of the dots also present a low symmetry and the central line associated with $S_z = 0$ is split by the electron-hole exchange interaction and linearly polarized along two orthogonal directions (see for instance QD2 in Fig. 2). This is the fine structure splitting usually observed in nonmagnetic QDs. An additional line, labeled (D), often appears on the low-energy side of the exciton PL spectra. It arises from a dark exciton ($|\uparrow_h \uparrow_e\rangle$ or $|\downarrow_h \downarrow_e\rangle$) which acquires some oscillator strength by a mixing with a bright exciton associated with the same Cr spin state [14]. This bright-dark mixing can be induced by the electron-hole exchange interaction in a confining potential of symmetry lower than C_{2v} [24].

III. PL INTENSITY DISTRIBUTION IN A CR-DOPED QD

In magnetic QDs, the PL intensity distribution on the different exciton lines is a probe of the spin state of the

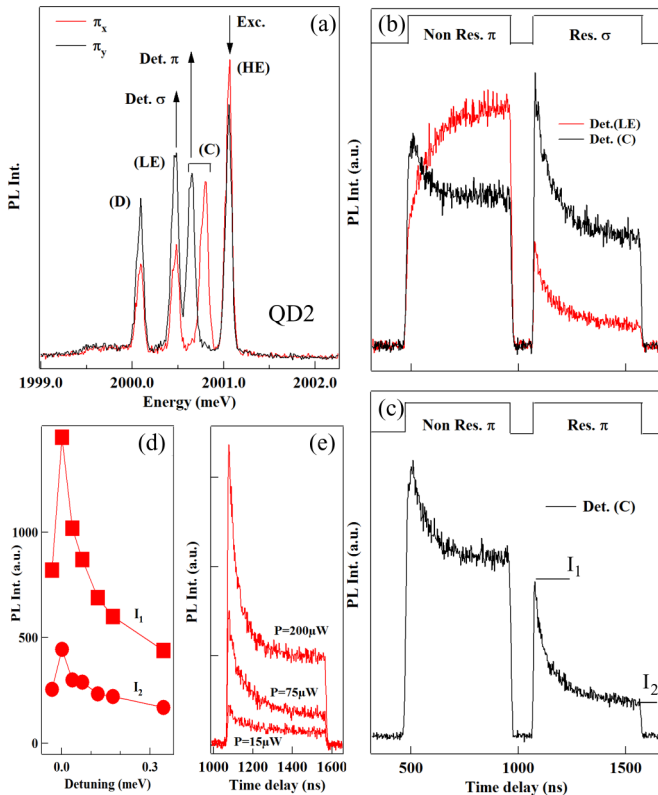


FIG. 2. (a) Linearly polarized PL spectra of the exciton in a Cr-doped QD (QD2) and configuration of the resonant excitation and detection in the optical pumping experiments. (b) and (c) resonant optical pumping experiment on QD2 for cross-circularly polarized excitation detection (b) and cross-linearly polarized excitation detection (c). (d) Energy detuning dependence of the resonant PL intensity (I_1 at the beginning and I_2 at the end of the pump pulse) detected in (C) for cross-linearly polarized excitation detection. (e) Excitation power dependence of the resonant PL transient detected in (C) for cross-linear excitation detection.

magnetic atom when the exciton recombines. For a Cr-doped QD, the exciton-Cr PL intensity distribution depends both on the thermalization on the spin states of the magnetic atom when the QD is empty and on the exciton-Cr spin relaxation during the lifetime of the exciton. In the absence of charge fluctuations in the QD, the first mechanism is only controlled by the interaction with acoustic phonons and can eventually lead to an effective spin temperature larger than the temperature of the lattice if nonequilibrium phonons are present in the system.

When an exciton is present in the QD, the spin dynamics results from carrier-Cr spin flip-flops and spin-phonon coupling. Under injection of spin polarized carriers, the carrier-Cr spin flip-flops can be responsible for an eventual optical orientation of the magnetic atom spin [4,25]. We show here that both the PL intensity distribution under nonresonant excitation and the fluorescence obtained under resonant excitation suggest an efficient spin transfer within the exciton-Cr complex from the spin states $S_z = \pm 1$ to $S_z = 0$. The excitation power dependence of the intensity distribution confirms that these spin transfers arise from carrier-Cr spin-flips.

A. PL intensity distribution under nonresonant excitation

Figure 1 presents the excitation power dependence of the PL of the exciton in a Cr-doped QD. After a nearly linear evolution at low excitation power all the X-Cr PL lines present a saturation at high excitation when a biexciton starts to be created in the QD [Fig. 1(b)]. The saturation is slightly faster for line (D) which is mainly a dark exciton. This is a consequence of its longer lifetime which results in a larger probability to form a biexciton. A detailed analysis of this measurement reveals that the ratio of the PL intensity of the central line and the low or high energy lines ($I_{(C)}/I_{(LE)}$ and $I_{(C)}/I_{(HE)}$) depend on the excitation power. With the increase of the excitation power we first observe a slow decrease of these ratio before they quickly reincrease at high excitation power.

The initial decrease of these ratio which corresponds to a slightly faster increase of the intensity of the two outer lines compared to the intensity of the central line, corresponds to an increase of the effective spin temperature of the Cr spin. The localized spins in a diluted magnetic semiconductor are coupled to the carrier reservoir through the exchange interaction and to the phonon reservoir through the spin lattice coupling. An efficient interaction with phonons is indeed expected for magnetic atoms with an orbital momentum, like Cr, which are sensitive to the fluctuation of their local strain environment (large spin-to-strain coupling). An increase of the effective spin temperature of the magnetic atoms is then the expected behavior when unpolarized carriers and/or acoustic phonons are optically injected in the QD [22]. The strong influence of the direct coupling of the localized spin of the Cr with nonequilibrium acoustic phonons generated during the optical excitation will be confirmed in the last part of this paper and is likely to be responsible for the observed spin heating.

The fast increase of the ratio of the PL intensities observed at high excitation power where the central line dominates the PL spectra [Fig. 1(a)] is more puzzling. It goes against the expected evolution for an increase of the Cr spin temperature at high excitation power. This evolution suggests an efficient transfer from the high energy states with $S_z = \pm 1$ to the low energy states with $S_z = 0$. This transfer is enhanced by the probability of the presence of an exciton in the QD. Some carrier-Cr spin-flips are then at the origin of this relaxation process towards $S_z = 0$.

B. Intensity distribution of the resonant PL

To confirm the presence of this spin transfer mechanism induced by the exciton in the QD, we analyzed the PL intensity distribution under resonant excitation. It was recently demonstrated that the spin of an individual Cr atom can be efficiently pumped under resonant optical excitation [21]. In these experiments, the initialization of the Cr spin which takes place in a few tens of ns was detected in the resonant PL of the QD emitted after a spin-flip of the exciton conserving the Cr spin. However, no specific spin-flip mechanisms were identified to explain this resonant optical pumping process.

In order to analyze more in detail the distribution of the resonant PL during the optical pumping process we used a two wavelength pump-probe experiment (see Fig. 2). A circularly polarized single mode laser (called *resonant pump*) tuned on resonance with an exciton-Cr line is used to pump the Cr

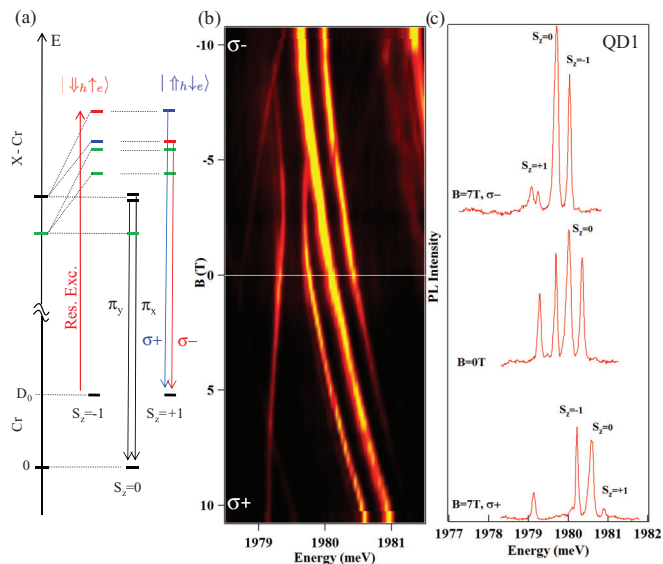


FIG. 3. (a) Diagram of the energy levels in a Cr-doped QD (Cr alone and exciton-Cr). Only the three low energy Cr spin states $S_z = 0$ and $S_z = \pm 1$ are presented. Both the bright excitons ($|\uparrow_h \downarrow_e\rangle$ in blue and $|\downarrow_h \uparrow_e\rangle$ in red) and the dark excitons ($|\uparrow_h \uparrow_e\rangle$ or $|\downarrow_h \downarrow_e\rangle$ in green) are presented. *Res. Exc.* stands for the energy of the laser used in the resonant optical pumping experiments. (b) PL intensity map of the magnetic field dependence of the exciton in QD1 in the Faraday configuration. (c) Circularly polarized PL spectra at $B_z = 0$ T and $B_z = 7$ T in $\sigma+$ and $\sigma-$ polarization.

spin (i.e., empty the spin state under resonant excitation). A second laser, which is here tuned on an excited state of the QD (called *probe*), injects high energy unpolarized excitons which relax toward the ground states of the QDs by emitting an avalanche of acoustic phonons. The interaction with the injected unpolarized carriers and/or acoustic phonons drives back the Cr to an effective spin temperature where the three ground states $S_z = 0$ and $S_z = \pm 1$ are populated [21].

Under circularly polarized resonant excitation of the high energy exciton-Cr line, a weak PL is observed in cross-circular polarization on the low energy bright exciton line after a spin-flip of the exciton conserving the Cr spin. In this experimental configuration the same spin state of the Cr is excited and detected [see the energy level diagram presented in Fig. 3(a)]. The intensity transient observed during the resonant PL [Fig. 2(b)] directly reflects the pumping of the Cr spin state under excitation ($S_z = +1$ or $S_z = -1$).

However, as presented in Fig. 2(b), during this resonant pumping process a luminescence is also observed on the central lines (linearly polarized bright excitons resulting from the mixing of $|0\rangle|\uparrow_h \downarrow_e\rangle$ and $|0\rangle|\downarrow_h \uparrow_e\rangle$). This resonant PL presents a transient with a similar time scale and amplitude as the one detected on the low energy bright exciton. This steady state PL intensity is strongly reduced under cross linearly polarized excitation and detection [Fig. 2(c)].

The central line in a Cr-doped QD is split by the electron-hole exchange interaction (long range and/or short range exchange interaction in the presence of valence band mixing)

and linearly polarized along two orthogonal directions. For a circularly polarized excitation on the high energy side of these transitions and for a cross-circularly polarized detection, a weak absorption in the acoustic phonon sideband [26] is expected to induce some resonant PL. However, the presence of the intensity transient due to the pumping of the resonantly excited spin states $S_z = \pm 1$ shows that there is also an efficient population transfer between the high energy bright excitons ($|+1\rangle|\uparrow_h \downarrow_e\rangle$ or $|-1\rangle|\downarrow_h \uparrow_e\rangle$) created during the resonant optical excitation and the lower energy bright exciton states ($|0\rangle|\downarrow_h \uparrow_e\rangle$ or $|0\rangle|\uparrow_h \downarrow_e\rangle$).

For a cross-linearly polarized excitation and detection, the absorption in the acoustic phonon side-band is strongly reduced. The pumping transient resulting from an absorption on the states $S_z = \pm 1$ and a transfer toward $S_z = 0$ dominates the resonant PL. This spin-flip transfer is confirmed by the excitation energy and power dependence of the resonant PL signal. The PL intensity on the central line presents a resonant behavior when scanning the pump laser around the high energy line [Fig. 2(d)]. As expected for an optical pumping process, the time scale of the PL transient is also significantly reduced with the increase of the excitation intensity [Fig. 2(e)].

This efficient transfer towards $S_z = 0$ during the resonant optical pumping process is also observed in the evolution of the PL intensity during the nonresonant probe (heating) pulse. As expected after a resonant pumping of the spin states $S_z = \pm 1$, their population re-increase during the nonresonant heating pulse. Simultaneously, a significant decrease of the intensity of the central line is observed both for a circularly or a linearly polarized detection [Figs. 2(b) and 2(c)]. This decrease corresponds to a decrease of the population of $S_z = 0$ during the heating process showing that a significant part of the Cr spin population has been transferred to $S_z = 0$ during the resonant optical pumping.

IV. MAGNETIC FIELD DEPENDENCE OF THE PL INTENSITY DISTRIBUTION IN A CR-DOPED QD

We have seen that the exciton-Cr dynamics significantly affects the intensity distribution in the PL of Cr-doped QDs at zero magnetic field. At high excitation power the intensity distribution no longer reflects a simple thermalization on the Cr spin states at the lattice temperature. This is also particularly true under magnetic field where the expected thermalization on the Zeeman split Cr spin states $S_z = \pm 1$ is not clear in most of the dots at the large excitation power needed to obtain a large enough PL signal [14].

At moderate excitation power, a variation under magnetic field of the intensity distribution between the high and low energy lines can however be observed in some of the Cr-doped QDs. As presented in Fig. 3, under a magnetic field applied along the QD growth axis, a maximum of PL intensity is observed on the high energy side of the exciton-Cr spectra in $\sigma-$ polarization and on the low energy side in $\sigma+$ polarization. This change in the intensity distribution is more or less pronounced from one dot to another [see also the case of QD3 in Fig. 4(b)] but always presents the same tendency. Such distribution, with a maximum of PL intensity on the high energy side in $\sigma-$ polarization (which shifts to low energy under $B_z > 0$) and on the low energy side in $\sigma+$ polarization,

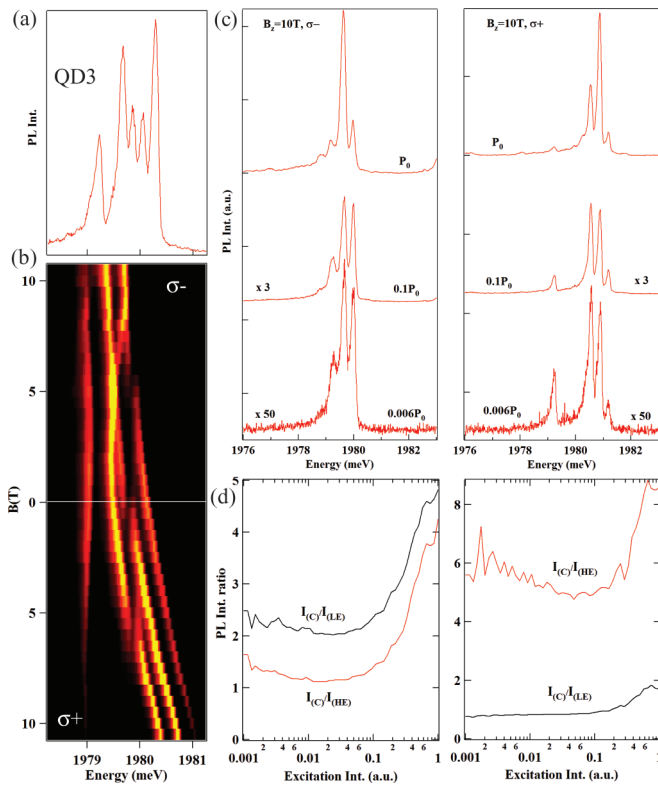


FIG. 4. (a) Zero magnetic field PL of the exciton-Cr complex in QD3 and (b) intensity map of the magnetic field dependence of the PL of QD3. (c) Excitation power dependence of the PL of QD3 at $B_z = 10$ T in σ^- (left) and σ^+ (right) polarization. (d) Corresponding excitation power dependence of the PL intensity ratios $I_{(C)}/I_{(LE)}$ and $I_{(C)}/I_{(HE)}$.

is identical to the one observed in singly Mn-doped CdTe/ZnTe QDs. In these systems, the hole-Mn exchange interaction is known to be antiferromagnetic [27] and approximately four times larger than the ferromagnetic electron-Mn exchange interaction.

Under a longitudinal magnetic field the Cr spin states $S_z = \pm 1$ in the empty QD are split by the Zeeman energy $g_{Cr} \mu_B B_z$ with a Lande factor $g_{Cr} \approx 2$. Among the Zeeman doublet $S_z = \pm 1$, the Cr spin thermalizes on the lowest energy Cr spin state $S_z = -1$ at low temperature. At moderate excitation power where the exciton-Cr PL intensity distribution is not dominated by the carriers-Cr spin-flips, this population distribution can be partially mapped on the exciton-Cr PL. When an unpolarized exciton is injected in the QD, the energy position of the most populated states with $S_z = -1$, on the high energy or the low energy side of the exciton PL spectra, depends on the sign of the exciton-Cr exchange interaction. This exchange interaction results from the sum of the electron-Cr and hole-Cr exchange interactions.

The electron-Cr coupling for carriers at the center of the Brillouin zone arises from the standard exchange interaction. It is then ferromagnetic and a value of $N_0\alpha$ around 0.2 eV is found for most of the transition metals incorporated in wide band gap II-VI compounds [28]. The exchange interaction with the electron spin is usually weaker than the exchange interaction with the holes spin which arises from the hybridization of

the d orbital of the magnetic atom and the p orbital of the host semiconductor, the so-called kinetic exchange.

The value of the exchange interaction with the holes resulting from a hybridization is strongly sensitive to the energy splitting between the $3d$ levels of the atom and the top of the valence band. This hybridization of course significantly depends on the considered transition metal element (i.e., filling of the $3d$ orbital) but also, for a given magnetic element, on the semiconductor host [29].

It has been demonstrated by Blinowski and Kacman [28,30] that the exchange interaction between a Cr atom ($3d^4$) with a Jahn-Teller distortion oriented along the [001] axis (z axis) and a heavy hole with a z component of its total angular momentum $J_z = \pm 3/2$ can be expressed in the form:

$$H_{ex} = -\frac{1}{3} S_z J_z B_4, \quad (1)$$

where B_N (with $N = 4$ for Cr) is given by

$$B_N = -\frac{V_{pd}^2}{S} \left[\frac{1}{\varepsilon_p + E_{N-1}^{S-1/2} - E_N^S} + \frac{1}{E_{N+1}^{S-1/2} - E_N^S - \varepsilon_p} \right] \quad (2)$$

with E_N^S the unperturbed energy of the d shell with N electrons and total spin S , V_{pd} the hybridization constant between the d orbital of the impurity and the p orbital of the semiconductor host, and ε_p the energy of the top of the valence band [28]. This Cr site orientation along the [001] axis corresponds to the CdTe/ZnTe QDs where a Cr atom can be optically detected. Such dots are characterized by a large biaxial strain which dominates the Jahn-Teller effect and orients the Cr spin along the QD growth axis [31].

In the expression (2) controlling the amplitude of the hole-Cr exchange, the first denominator corresponds to the energy e_1 required to transfer an electron from the d shell of the Cr atom to the valence band reducing the total spin from S to $S - 1/2$ (and reducing the number of electrons in the d shell from N to $N - 1$). The denominator of the second term is the energy e_2 required to transfer an electron from the top of the valence band to the d shell also with a reduction by $1/2$ of the total spin (and an increase of the number of electrons in the d shell from N to $N + 1$). This last energy e_2 includes the electron-electron exchange interaction in the d shell (at the origin of Hund rule) and is then large (a few eV) and always positive.

The sign of B_4 controls the sign of the hole-Cr kinetic exchange interaction: A negative B_4 corresponds to an antiferromagnetic interaction whereas a positive B_4 will give rise to a ferromagnetic interaction. If e_1 is negative ($E_N^S - E_{N-1}^{S-1/2} > \varepsilon_p$) and $1/e_1 < -1/e_2$, B_4 is positive. The donor transition Cr^{2+} to Cr^{3+} is within the band gap of the semiconductor and the hole-Cr exchange interaction is ferromagnetic. This is the situation reported until now for all the studied bulk II-VI compounds containing diluted Cr atoms [32]. In particular, Cr-doped bulk ZnTe exhibits a large ferromagnetic exchange interaction. This is consistent with the optical observation of the Cr^{2+} to Cr^{3+} donor transition about 0.2 eV above the top of the valence band in ZnTe [33].

For a positive value of e_1 ($E_N^S - E_{N-1}^{S-1/2} < \varepsilon_p$), B_4 is negative and the hole-Cr exchange interaction is antiferromagnetic. This corresponds to a donor transition Cr^{2+} to Cr^{3+} within the

valence band. According to equation (2), a slight change of the value of e_1 around 0 can abruptly change the hole-Cr exchange from a large ferromagnetic to a large antiferromagnetic value. However, one should note that the calculations leading to the expression of the kinetic exchange interaction (1) contain two important approximations. First, the influence of the crystal field and strain modified crystal field on the magnetic atom d orbital is neglected. Secondly, the model is based on a perturbation approach which is not particularly well adapted when e_1 is close to zero as expected for Cr in CdTe or ZnTe.

The hole-Cr exchange interaction has never been measured in bulk CdTe. However, the energy level of a transition-metal impurity does not significantly change between materials with common anion [29]. The valence band offset between ZnTe and CdTe being around 0.1 eV [34] one could also expect that the Cr donor transition in bulk CdTe could be very close but slightly above the top of the valence band. This should give rise to a ferromagnetic hole-Cr exchange interaction as observed for Cr-doped ZnTe. However, whereas the acceptor transition Cr^{2+} to Cr^{1+} has clearly been optically identified in bulk CdTe, the donor level Cr^{2+} to Cr^{3+} has never been observed suggesting, following Ref. [35], that it could be resonant with the valence band. The resulting hole-Cr exchange interaction would then be large an antiferromagnetic.

The intensity distribution observed under magnetic field in the studied Cr-doped QDs (see Figs. 3 and 4) shows that the exciton-Cr state $| -1 \rangle | \downarrow_h \uparrow_e \rangle$ is at high energy whereas the state $| -1 \rangle | \uparrow_h \downarrow_e \rangle$ is at low energy. This corresponds, for a CdTe/ZnTe QD, to an antiferromagnetic exchange interaction between the heavy-hole and the Cr spins. The sign of this interaction could however be different in bulk CdTe. For a CdTe QD in a ZnTe barrier, the large biaxial strain can decrease the energy of the ground heavy hole levels, e_1 can become negative, and the resulting exchange interaction antiferromagnetic. The strain induced modification of the crystal field can also significantly influence the energy level of the d orbital of the Cr and modify the kinetic exchange with the nearby hole spins at the top of the valence band. A more detailed model should be developed to properly describe the influence of the hybridization in these strained and confined systems where the d levels of the magnetic atom are close in energy with the edge of the valence band.

As observed at zero field, the PL intensity distribution under magnetic field is also strongly perturbed by the variation of the excitation power. This is presented in Figs. 4(c) and 4(d) for QD3. At high excitation power the distribution intensity observed under magnetic field is far from a simple thermalization on the Cr spin states split by the magnetic anisotropy and the Zeeman energy. The excitation power intensity dependence reported in Fig. 4(d) confirms the behavior observed at zero field with a significant increase of the population of the spin state $S_z = 0$ (central line) induced by the presence of the exciton in the QD at high excitation power. At high excitation power and under $B_z = 10$ T [Fig. 4(c)] the PL is strongly dominated by the central line in both circular polarizations. This can prevent the clear observation of the expected thermalization on the Zeeman split Cr spin states $S_z = \pm 1$. However, a careful look at the high and low energy lines shows that the tendency in the PL intensity distribution always reflects the antiferromagnetic interaction of the hole and Cr spins.

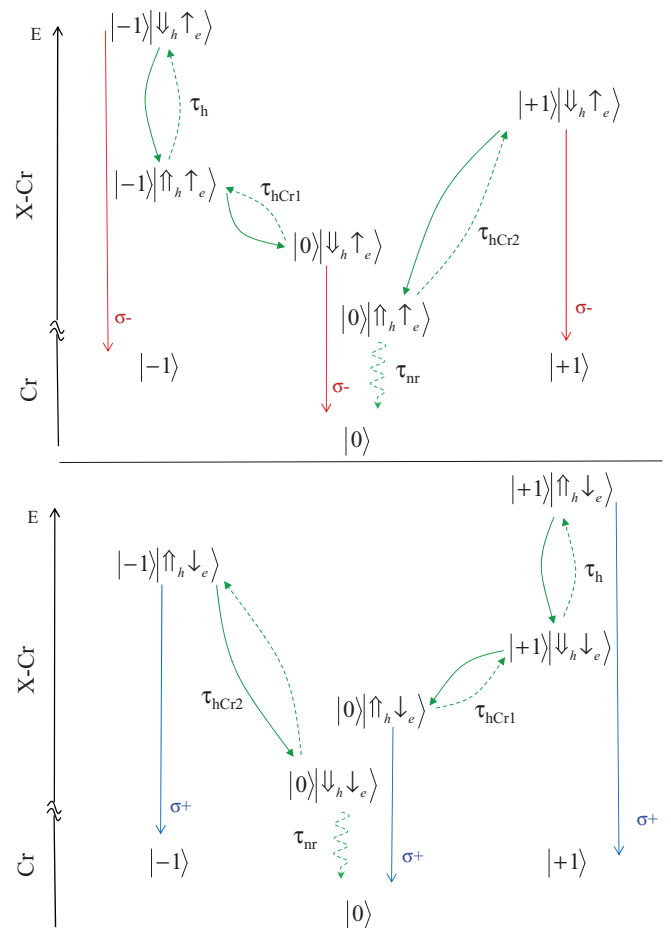


FIG. 5. Proposed spin relaxation paths within the exciton-Cr complex (X-Cr) for an excitation of the bright exciton $| \downarrow_h \uparrow_e \rangle$ in σ^- polarization (top) and of the bright exciton $| \uparrow_h \downarrow_e \rangle$ in σ^+ polarization (bottom). τ_h is the spin flip time of the hole, τ_{hCr1} is a hole-Cr flip-flop times, and τ_{nr} is the nonradiative recombination time of the dark excitons.

V. EXCITON-CR SPIN RELAXATION INDUCED BY HOLE-CR FLIP-FLOPS

The analysis of the PL intensity distribution in Cr-doped CdTe QDs shows that (i) the hole-Cr exchange interaction is antiferromagnetic and that (ii) a fast carriers-Cr spin dynamics induces some spin transfer from $S_z = \pm 1$ to $S_z = 0$ within the exciton-Cr complex. Recently, efficient hole-Mn flip-flops were identified in positively charged Mn-doped QDs as the main source of spin relaxation for a confined hole-Mn complex and also observed in the resonant PL of the exciton in a neutral Mn-doped QD [36]. It was shown that these flip-flops are induced by an interplay of the carriers-magnetic atom exchange interaction and the coupling with acoustic phonons. A similar spin relaxation process involving simultaneous spin-flip of the hole and the Cr spins should also exist in neutral Cr-doped QDs.

A fast hole-Cr flip-flop could indeed explain an efficient transfer of population from the exciton-Cr levels $S_z = \pm 1$ towards the low energy states $S_z = 0$. The proposed relaxation path is illustrated in the energy level scheme presented in Fig. 5 which displays the possible relaxation channels involving a

hole-Cr flip-flop for an initial excitation of the bright excitons coupled with $S_z = \pm 1$.

Under linearly polarized nonresonant excitation, the different spin states of the bright ($|\downarrow_h \uparrow_e\rangle$ and $|\uparrow_h \downarrow_e\rangle$) and dark ($|\uparrow_h \uparrow_e\rangle$ and $|\downarrow_h \downarrow_e\rangle$) excitons are populated with the same probability. Starting from the low energy bright excitons $|+1\rangle|\downarrow_h \uparrow_e\rangle$ or $|-1\rangle|\uparrow_h \downarrow_e\rangle$, a hole-Cr flip-flop with conservation of the electron spin can directly transfer the population towards the dark excitons associated with $S_z = 0$ with a spin flip time τ_{hCr2} . With the same mechanism, a direct transfer is possible from the low energy dark excitons $|+1\rangle|\downarrow_h \downarrow_e\rangle$ or $|-1\rangle|\uparrow_h \uparrow_e\rangle$, to the bright excitons associated with $S_z = 0$ with a spin flip time τ_{hCr1} (see Fig. 5).

Starting from the high energy bright excitons $|+1\rangle|\uparrow_h \downarrow_e\rangle$ or $|-1\rangle|\downarrow_h \uparrow_e\rangle$, a hole-Cr flip-flop is unlikely as it would involve a transfer toward the high energy Cr spin states $S_z = \pm 2$. However, a spin flip of the hole with characteristic time τ_h conserving the spin of the Cr can induce a transfer to the low energy dark excitons $|+1\rangle|\downarrow_h \downarrow_e\rangle$ or $|-1\rangle|\uparrow_h \uparrow_e\rangle$. Such spin-flip from a bright to a dark exciton can occur in QDs in a timescale of a few nanoseconds [37]. A hole-Cr flip-flop in a timescale τ_{hCr1} can then transfer the population from these dark excitons to the $S_z = 0$ bright exciton which then recombines optically (see Fig. 5).

From the high energy dark excitons $|+1\rangle|\uparrow_h \uparrow_e\rangle$ or $|-1\rangle|\downarrow_h \downarrow_e\rangle$ a hole-Cr flip-flop is also unlikely (transfer toward the high energy Cr spin states $S_z = \pm 2$). However these states are coupled by a hole spin-flip to the nearby low energy bright excitons $|+1\rangle|\downarrow_h \uparrow_e\rangle$ or $|-1\rangle|\uparrow_h \downarrow_e\rangle$ and can then follow this path to be transferred towards $S_z = 0$.

The spin relaxation channels involving a transfer from the dark exciton with $S_z = \pm 1$ to the lower energy bright excitons $S_z = 0$ are made irreversible by the fast (≈ 250 ps) radiative recombination of the final low energy exciton state. This unusual situation with some of the bright excitons at lower energy than the dark ones can induce an out of equilibrium distribution on the Cr spin states with an enhanced population of the $S_z = 0$ ground state. The transfer mechanism involving a hole-Cr flip-flop is enhanced by the increase of the probability of presence of an exciton in the QD. As observed in the excitation power dependence of the nonresonant PL, these processes only affect the distribution of the PL intensity at high excitation power. At low excitation power, the QD is empty most of the time, the exciton really acts as a probe, and the intensity distribution is mainly controlled by the Cr spin temperature driven by the interaction with phonons (equilibrium phonons at the temperature of the lattice and nonequilibrium phonons generated during the optical excitation).

Under resonant excitation on the high energy lines of X-Cr, a spin flip of the hole followed by a fast hole-Cr flip-flops can also explain the observed transfer of excitation toward the bright excitons associated with $S_z = 0$. This process which efficiently changes the Cr spin is likely to be the main source for the resonant optical pumping demonstrated in Cr-doped QDs [21].

A. Phonon induced hole-Cr flip-flops

The timescale of the hole-Cr flip-flops in a Cr-doped QD induced by the interaction with the continuum of bulk

acoustic phonons can be estimated using the Fermi golden rule. The spin-flip process that we consider here is based on the interplay of the hole-magnetic atom exchange interaction and the interaction with the strain field of acoustic phonons [36]. Similar models, combining exchange interaction and coupling with acoustic phonons, were developed to explain the exciton spin relaxation in QDs [38,39].

Let us consider for instance the two exciton-Cr states $|+1\rangle|\downarrow_h; \downarrow_e\rangle$ and $|0\rangle|\uparrow_h; \downarrow_e\rangle$ that can be coupled via a hole-Cr flip-flop. The nondiagonal terms of the hole-Cr exchange interaction couples the heavy-holes and light-holes exciton levels separated in energy by Δ_{lh} through a hole-Cr flip-flop. To the first order in I_{hCr}/Δ_{lh} , the two perturbed heavy-hole exciton ground states can be written:

$$\begin{aligned} | +1 \rangle | \widetilde{\downarrow_h; \downarrow_e} \rangle &= | +1 \rangle | \downarrow_h; \downarrow_e \rangle - \frac{\sqrt{18} I_{hCr}}{2 \Delta_{lh}} | 0 \rangle | \downarrow_h; \downarrow_e \rangle \\ | 0 \rangle | \widetilde{\uparrow_h; \downarrow_e} \rangle &= | 0 \rangle | \uparrow_h; \downarrow_e \rangle - \frac{\sqrt{18} I_{hCr}}{2 \Delta_{lh}} | +1 \rangle | \uparrow_h; \downarrow_e \rangle, \end{aligned} \quad (3)$$

where we neglect the exchange energy shifts of the exciton-Cr levels much smaller than Δ_{lh} .

The strain field produced by acoustic phonon vibrations couples the perturbed exciton-Cr states through the Hamiltonian term:

$$\langle \downarrow_h; \downarrow_e | \widetilde{\downarrow_h; \downarrow_e} | \langle +1 | H_{BP} | 0 \rangle | \widetilde{\uparrow_h; \downarrow_e} \rangle = 2 \times \left(-\frac{\sqrt{18} I_{hCr}}{2 \Delta_{lh}} \right) \times r^* \quad (4)$$

with $r = \sqrt{3}/2b(\epsilon_{xx} - \epsilon_{yy}) - id\epsilon_{xy}$ a strain-dependent non-diagonal term of the Bir-Pikus Hamiltonian H_{BP} [40]. The coupling of these exciton-Cr states is then a result of an interplay between the hole-Cr exchange interaction and the strain field of acoustic phonons.

In analogy with the model developed in Ref. [36] to describe hole-Mn flip-flops in positively charged Mn-doped QDs, the decay rate associated with the emission of phonons which is deduced from the Fermi golden rule and the matrix element (4) can be written:

$$\begin{aligned} \tau^{-1} &= \sum_{\lambda} \frac{18}{(2\pi)^2} \left(\frac{I_{hMn}}{\Delta_{lh}} \right)^2 \left(\frac{\omega_0}{c_{\lambda}} \right)^3 \frac{1}{2\hbar\rho c_{\lambda}^2} \frac{\pi}{4} (3b^2 + d^2) \\ &\times (n_B(\omega_0) + 1) \int_0^{\pi} d\theta \sin\theta |\mathcal{F}_{\lambda}(\omega_0, \theta)|^2 G_{\lambda}(\theta), \end{aligned} \quad (5)$$

where the summation is taken over the acoustic phonon branches λ (one longitudinal l and two transverse t_1, t_2) of corresponding sound velocity c_{λ} . The geometrical form factors for each phonon branch appearing in Eq. (5), $G_{\lambda}(\theta)$, are given by $G_l(\theta) = \sin^4 \theta$, $G_{t_1}(\theta) = \sin^2 \theta \cos^2 \theta$ and $G_{t_2}(\theta) = \sin^2 \theta$.

Numerical calculation of the hole-Cr spin-flip time in a CdTe QD are presented in Fig. 6. We use in the calculation a Gaussian wave function for the hole with in-plane and z -direction parameters l_{\perp} and l_z , respectively, the material parameters of CdTe and typical parameters of self-assembled CdTe/ZnTe QDs are listed in Table II of the Appendix.

The calculated spin relaxation time strongly depends on the energy splitting between the exciton-Cr states involved in the hole-Cr flip-flops [Fig. 6(a)]. This dependence on the

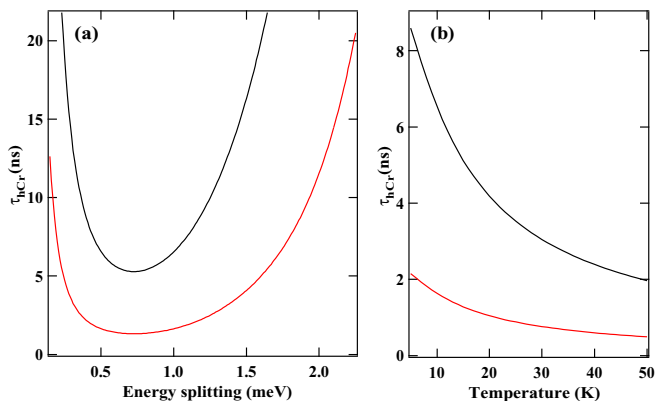


FIG. 6. (a) Relaxation time τ_{hCr} between the states $|+1\rangle|\downarrow_h; \downarrow_e\rangle$ and $|0\rangle|\uparrow_h; \downarrow_e\rangle$ (or $|-1\rangle|\uparrow_h; \uparrow_e\rangle$ and $|0\rangle|\downarrow_h; \uparrow_e\rangle$) as a function of the energy splitting between those states, calculated at a temperature $T = 10$ K with a Gaussian hole wave function (parameters $l_z = 1.25$ nm and $l_\perp = 3$ nm) and $\Delta_{lh} = 25$ meV (red), $\Delta_{lh} = 50$ meV (black). The other QD parameters are listed in Table I of the Appendix. The CdTe parameters used in the calculation can be found in Table II of the Appendix. (b) Temperature variation of the relaxation time for an energy splitting $E = 1$ meV and $\Delta_{lh} = 25$ meV (red), $\Delta_{lh} = 50$ meV (black).

high energy side is controlled by the size of the hole wave function which limits the wave vector of the acoustic phonons that can interact with the hole. The calculated spin-flip time can be easily in the few nanosecond range for an energy splitting between 0.5 meV and 2 meV. In the studied Cr-doped QDs, the splitting between the low energy dark excitons states $|+1\rangle|\downarrow_h\downarrow_e\rangle$ or $|-1\rangle|\uparrow_h\uparrow_e\rangle$ and the bright excitons with $S_z = 0$, which are coupled by a hole-Cr flip-flop, is typically in the 1 meV range. A spin-flip time in a few ns range can then be expected.

For the low energy bright excitons $|+1\rangle|\downarrow_h\uparrow_e\rangle$ or $|-1\rangle|\uparrow_h\downarrow_e\rangle$ and the dark excitons states with $S_z = 0$ also coupled by hole-Cr flip-flops, their energy splitting is larger than 3 meV and the spin-flip rates are expected to be significantly reduced. For the high energy Cr spins states Cr, $S_z = \pm 2$, the energy splitting is typically larger than 10 meV and the corresponding flip-flops induced by the discussed mechanism can be neglected.

The estimated hole-Cr flip-flop time is also strongly sensitive to the effective energy splitting between heavy-hole and light-hole Δ_{lh} . This simple parameter is used in our model for an effective description of the valence band mixing. It can describe complex effects such as a coupling of the confined heavy-hole with ground state light-holes in the barriers [41] or effective reduction of heavy-hole/light-hole splitting due to a presence of a dense manifold of heavy-hole like QD states lying between the confined heavy-hole and light-hole levels [42]. This parameter can significantly change from dot to dot and modify the hole-Cr flip-flop time.

The calculated hole-Cr flip-flop rate also depends on the temperature through the stimulated emission of acoustic phonons. For an energy splitting of 1 meV the spin flip rate involving the emission of phonons is increased by a factor of about four by increasing the temperature from 5 K to 50 K [Fig. 6(b)]. Such enhancement of the hole-Cr spin-flip

rate could not only be induced by an increase of the lattice temperature but also, as in our experiments, by the presence of nonequilibrium phonons that are generated by the optical excitation inside or in the vicinity of the QD.

B. Calculated PL intensity distribution in a Cr-doped QD

To confirm that the hole-Cr spin-flip process we described in the previous section is the source of the excitation power dependence of the PL intensity distribution observed in Cr-doped QDs, we developed a rate equation model for the population of the different energy levels. We calculated the steady state population of the twenty exciton-Cr states and the five biexciton states in the excited state of the QD and the five Cr spin states in the ground state by solving numerically the master equation for the corresponding 30×30 density matrix ρ . The time evolution of the density matrix of this multilevel opened quantum system can be described by the Lindblad formalism and is given by

$$\frac{\partial \rho}{\partial t} = \frac{-i}{\hbar} [\mathcal{H}, \rho] + L\rho, \quad (6)$$

where \mathcal{H} is the Hamiltonian of the complete system (X-Cr, X^2 -Cr, and Cr alone) and $L\rho$ describes the coupling or decay channels resulting from an interaction with the environment [43–45].

The energy levels of the Cr in an empty dot are controlled by the magnetic anisotropy $D_0 S_z^2$. The X-Cr Hamiltonian contains the energy of the Cr spin states, the carriers-Cr exchange interaction, the electron-hole exchange interaction in a confining potential of low symmetry (see appendix for details) and the structure of the valence band including possible heavy-hole/light-hole mixing. We restrict here to the heavy-hole subspace and introduce the valence band mixing with pseudo spin operators (see appendix). D_0 in the Cr Hamiltonian and the parameters in the X-Cr Hamiltonian cannot be precisely extracted from the magneto-optics PL measurements. For a qualitative description of the observed spin dynamics, we use typical Cr-doped QD parameters that give good order of magnitudes for the exciton-Cr splitting and the position of the main anticrossing (see Fig. 9 in the Appendix). Details of the spin effective Hamiltonian and the list of the parameters used in the calculation are presented in the Appendix.

To qualitatively describe the main feature of the spin dynamics in Cr-doped dots we take into account a spin relaxation of the Cr (alone or in the exchange field of the exciton or the biexciton), τ_{Cr} , describing relaxation channels involving a change of the Cr spin by one unit. We also include a spin-flip of the heavy-hole with a characteristic time τ_h . Relaxation channels involving the hole-Cr flip-flops are introduced between the Cr spin states $S_z = \pm 1$ and $S_z = 0$ with characteristic times $\tau_{hCr1} = 2$ ns for the low energy dark excitons with $S_z = \pm 1$ towards the bright exciton with $S_z = 0$ and a longer relaxation time $\tau_{hCr2} = 20$ ns for the low energy bright exciton with $S_z = \pm 1$ towards the dark exciton with $S_z = 0$ separated by a larger energy splitting (see Fig. 5). This flip-flop process is neglected for the spin states $S_z = \pm 2$ shifted to much higher energy.

We considered that the cw optical excitation simultaneously creates bright and dark excitons with a generation time $4\tau_g$

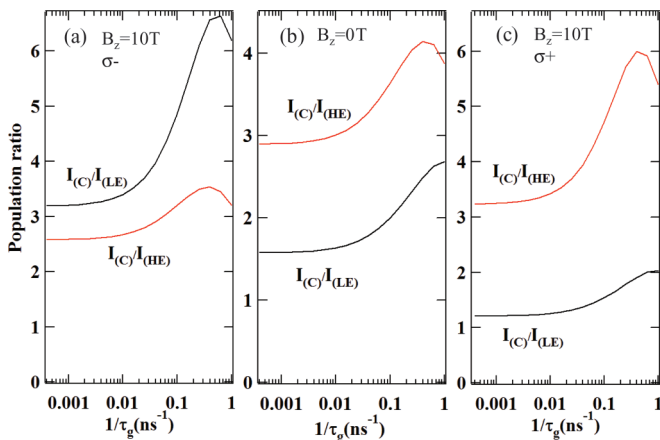


FIG. 7. Calculated excitation power dependence of the population ratios $I_{(C)}/I_{(HE)}$ and $I_{(C)}/I_{(LE)}$ at (a) $B_z = 10$ T in $\sigma-$ polarization ($\rho_{(0)|\downarrow_h, \uparrow_e}/\rho_{(-1)|\downarrow_h, \uparrow_e}$ and $\rho_{(0)|\downarrow_h, \uparrow_e}/\rho_{(+1)|\downarrow_h, \uparrow_e}$, respectively), at (b) $B_z = 0$ T and at (c) $B_z = 10$ T in $\sigma+$ polarization ($\rho_{(0)|\uparrow_h, \downarrow_e}/\rho_{(+1)|\uparrow_h, \downarrow_e}$ and $\rho_{(0)|\uparrow_h, \downarrow_e}/\rho_{(-1)|\uparrow_h, \downarrow_e}$, respectively). The parameters used in the model are $\tau_b = 0.25$ ns, $\tau_d = 20$ ns, $\tau_h = 10$ ns, $\tau_{Cr} = 50$ ns, $\tau_{hCr1} = 2$ ns, and $\tau_{hCr2} = 20$ ns. The QD parameters are listed in Table I of the Appendix.

(generation rate $\Gamma_g/4$). They recombine with a rate $1/\tau_b$ and $1/\tau_d$, respectively. When a biexciton is present in the QD, we only consider a recombination with a rate $1/\tau_b$ and possible spin-flips of the Cr with a characteristic time τ_{Cr} . Hole-Cr flip-flops are unlikely within the biexciton as they would drive the biexciton to a much higher energy excited state with two parallel hole spins.

The transition rates $\Gamma_{\gamma \rightarrow \gamma'}$ between the different states of the Cr, X-Cr, or X^2 -Cr depend on their energy separation $E_{\gamma\gamma'} = E_{\gamma'} - E_{\gamma}$. Here we use $\Gamma_{\gamma \rightarrow \gamma'} = 1/\tau_i$ if $E_{\gamma\gamma'} < 0$ and $\Gamma_{\gamma \rightarrow \gamma'} = 1/\tau_i e^{-E_{\gamma\gamma'}/k_B T_{\text{eff}}}$ if $E_{\gamma\gamma'} > 0$ [10,37]. This accounts for a thermalization among the 5 Cr levels, the 5 X^2 -Cr levels and the 20 X-Cr levels with an effective spin temperature T_{eff} . The optical excitation ($\tau_g = 1/\Gamma_g$), the exciton recombination (τ_b (bright) and τ_d (dark)), the hole spin relaxation (τ_h) and the Cr spin relaxation terms (τ_{Cr} , τ_{hCr1} , τ_{hCr2}) producing a population transfer from level j to level i are described by Lindblad terms

$$L_{j \rightarrow i} \rho = 1/(2\tau_{j \rightarrow i})(2|i\rangle\langle j|\rho|j\rangle\langle i| - \rho|j\rangle\langle j| - |j\rangle\langle j|\rho), \quad (7)$$

where $\tau_{j \rightarrow i}$ is the relaxation time from level j to level i [46].

Figure 7 presents the calculated excitation power dependence of the ratio of the population of the exciton-Cr states $\rho_{(0)|\downarrow_h, \uparrow_e}/\rho_{(-1)|\downarrow_h, \uparrow_e}$ ($I_{(C)}/I_{(HE)}$) and $\rho_{(0)|\downarrow_h, \uparrow_e}/\rho_{(+1)|\downarrow_h, \uparrow_e}$ ($I_{(C)}/I_{(LE)}$) at zero field and under a longitudinal magnetic field. As observed in the experiments, this ratio increases at high excitation intensity. This is due to the transfer from $S_z = \pm 1$ towards $S_z = 0$ described in the model by τ_{hCr1} and τ_{hCr2} . However this model is unable to reproduce the initial decrease of this ratio observed at low excitation power as it does not include an increase of the effective spin temperature of the Cr induced by the optical excitation. Instead, a stable effective spin temperature $T_{\text{eff}} = 40$ K larger than the lattice temperature is used in the model.

Under nonresonant excitation, the creation of the dark excitons $|+1\rangle|\downarrow_h \downarrow_e\rangle$ or $|-1\rangle|\uparrow_h \uparrow_e\rangle$ followed by a hole-Cr flip-flop and a fast optical recombination of the bright exciton is the main source for an irreversible spin transfer from $S_z = \pm 1$ to $S_z = 0$. The overall result of this process is an increase of the population of $S_z = 0$ with the optical excitation intensity when the transfer time becomes faster than the direct phonon induced relaxation of the Cr spin described by τ_{Cr} . The exciton induced spin transfer is attenuated when the QD starts to be significantly occupied by a biexciton as the hole-Cr flip-flops are forbidden within the biexciton. This is observed in the experiments (see Figs. 1 and 4) as well as in the model at high excitation power (Fig. 7).

Even if the values of the intensity ratios are slightly modified, a similar behavior is observed under magnetic field where the PL of the central line ($S_z = 0$) strongly dominates the emission spectra at high excitation power. Under magnetic field, the calculated evolution of the intensity ratio are also in good qualitative agreement with the experiments [see the experiments and calculations under $B_z = 10$ T in Figs. 4(d) and 7, respectively].

The PL observed from $S_z = 0$ under resonant excitation on the high energy line of X-Cr can also be explained by the presence of these efficient hole-Cr flip-flops. Under resonant excitation on the high energy line, the transition is optically cycled until a spin flip of the hole occurs. This spin-flip conserves the Cr spin and drives the system towards a dark exciton state. Then, a hole-Cr flip-flop can occur transferring the exciton to a bright state with $S_z = 0$ which recombines in a few tens of ps leaving the Cr in the spin state $S_z = 0$. The calculated hole-Cr flip-flop rates (Fig. 6) are consistent with the time scale of the observed pumping transients under resonant excitation (Fig. 2) confirming that the hole-Cr flip-flops are the main source of spin flips responsible for the resonant optical pumping of the Cr spin. The direct observation of a population transfer from $S_z = \pm 1$ to $S_z = 0$ in different experiments (nonresonant PL and resonant PL) is a clear evidence of the presence of this efficient hole-Cr flip-flop process.

VI. CR SPIN HEATING BY NONEQUILIBRIUM ACOUSTIC PHONONS

So far we have discussed the influence of the carrier-Cr spin-spin interaction on the PL intensity distribution in Cr-doped QDs. The resulting spin dynamics is dominated at high excitation power by hole-Cr flip-flops. The spin dynamics of an isolated magnetic atom in a semiconductor host is also sensitive to the interaction with acoustic phonons (spin lattice coupling). This is particularly important for a Cr atom which has an orbital momentum and is then expected to be sensitive to the local modification of the crystal field induced by fluctuating strain produced by acoustic phonons.

To evidence the interaction of the Cr spin with acoustic phonons we used a modified version of the two wavelength pump-probe experiment where carriers are not injected in the investigated QD during the probe pulse. Two configurations of pump-probe experiments were tested: a probe pulse a few μm away from the investigated Cr-doped QD or a probe pulse tuned to an energy close the ground state of the dot where there is no absorption in the investigated QD.

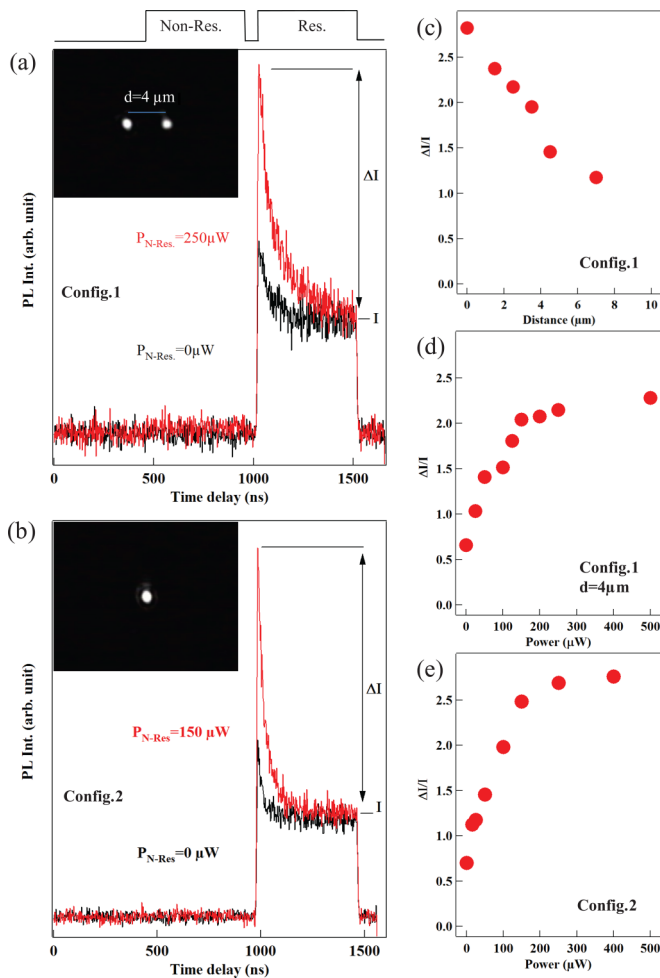


FIG. 8. Two wavelength pump-probe experiments performed on QD2. (a) Configuration 1: PL transients recorded for a probe laser tuned on an excited state of the dot and at $d = 4 \mu m$ from the dot. Red: probe on; black: probe off. (b) Configuration 2: PL transient recorded for overlapped pump and probe and a for probe laser at $E_{probe} = 2014$ meV, close to the resonant laser ($E_{pump} = 2001$, 1 meV); red: probe on; black: probe off. (c) Evolution of the pumping transient intensity as a function of the distance between the probe laser and the dot. (d) Evolution of the pumping transient intensity as a function of the probe power, for a probe laser at $d = 4 \mu m$ from the dot. (e) Evolution of the pumping transient intensity as a function of the probe power for a probe laser at $E_{probe} = 2014$ meV.

The results of these two experiments are summarized in Fig. 8. We first shift the probe laser away from the investigated Cr-doped QD and analyze the resonant optical pumping signal as a function of the distance and intensity of the probe pulse. The time resolved resonant PL obtained during a pump-probe sequence is presented in Fig. 8(a) for a distance $d = 4 \mu m$, a resonant excitation on the high energy line, and a cross-circularly polarized detection on the low energy line (excitation and detection of the same Cr spin state $S_z = +1$ or $S_z = -1$). At this distance, the probability for the optically created carriers to reach the QD is very weak and no luminescence is observed during the probe pulse. However, the amplitude of the resonant optical pumping transient significantly changes with the power of the probe pulse. When the probe is off,

the amplitude of the pumping transient is weak and controlled by the partial relaxation of the Cr spin during the dark time between two resonant pump pulses [21]. The amplitude of the transient significantly increases when the probe laser is switched on. The amplitude of the pumping transient is initially controlled by the intensity of the probe pulse before it saturates at high probe excitation power [Fig. 8(d)]. This shows that even if no carriers are injected in the QD, a heating of the Cr spin is induced by the probe pulse. For a given probe intensity, the amplitude of the transient progressively decreases with the increase of the distance between the QD and the probe spot [Fig. 8(c)].

A similar spin heating process is obtained when the pump and the probe are both at the Cr-doped QD position but the wavelength of the probe is tuned at an energy lower than the first excited state and slightly above the absorption in the acoustic phonon side band of the ground state (transparent window of the QD). As presented in Fig. 8(b) no significant PL is observed during the probe pulse. However, the amplitude of the pumping transient observed during the pump pulse depends on the probe intensity. The amplitude of the pumping transients saturates at high probe intensity [Fig. 8(e)].

In these two experimental configurations, even if carriers are not injected in the Cr-doped dot, the laser light being absorbed in the CdTe layer it generates photocarriers with excess kinetic energy. During their energy relaxation, nonequilibrium phonons are generated and propagate away from the probe laser spot (see submicron spots in the insets of Fig. 8). These phonons are not in equilibrium with the lattice temperature and no energy shift of the PL lines are observed under these experimental conditions. The heating of the Cr spin results from the direct interaction with these acoustic phonons [47] generated within the probe laser spot that can propagate across the sample. The observed decrease of the heating efficiency with the increase of the pump-probe distance is consistent with the expected decrease of the phonon flux that can reach the studied Cr atom as the punctual phonon source is moved away.

VII. CONCLUSION

We identified and modeled an efficient spin relaxation mechanism for a Cr spin in the exchange field of an exciton which transfers the Cr spin population from $S_z = \pm 1$ to $S_z = 0$. This spin relaxation, based on an interplay of the hole-Cr exchange interaction and the interaction with acoustic phonons, significantly affects the excitation power dependence of the PL intensity distribution. An analysis of the magnetic field dependence of the intensity distribution at moderate excitation power shows that the hole-Cr exchange interaction is antiferromagnetic. Considering this antiferromagnetic hole-Cr exchange interaction, the presence of the hole-Cr flip-flops with a few ns timescale can qualitatively explain (i) the excitation power dependence of the PL intensity distribution, (ii) the optical pumping of the Cr spin observed under resonant excitation, and (iii) the distribution of the PL obtained under resonant excitation. We also demonstrated that an isolated Cr spin is sensitive to nonequilibrium phonons generated during the optical excitation. This ensemble of experiments show that for a practical use of this single spin system, particular

care should be given to the optical excitation conditions. Nevertheless, the large spin-phonon coupling and the possible optical control of the spin makes Cr a promising platform to study the interaction of the $\{+1; -1\}$ Cr spin *qubit* with surface acoustic waves (phonons propagating at the surface of a sample) which are proposed as efficient quantum bus between different kinds of *qubits* [48].

ACKNOWLEDGMENTS

This work was realized in the framework of the Commissariat à l’Energie Atomique et aux Energies Alternatives (Institut Nanosciences et Cryogénie)/Centre National de la Recherche Scientifique (Institut Néel) joint research team NanoPhysique et Semi-Conducteurs. The work in Grenoble was supported by the French ANR project MechaSpin (ANR-17-CE24-0024) and CNRS PICS contract number 7463. The work in Tsukuba has partially been supported by the Grants-in-Aid for Scientific Research on Innovative Areas “Science of Hybrid Quantum Systems” and for challenging Exploratory Research.

APPENDIX A: SPIN HAMILTONIAN AND PARAMETERS OF CR-DOPED QDS

In this Appendix we present in more details the different parts of the spin effective Hamiltonian used in this paper to describe the PL spectra and the spin dynamics of CdTe/ZnTe Cr-doped QDs and give order of magnitude of the correspond-

ing QDs and material parameters. For the Cr alone in an empty QD, we take into account the magnetic anisotropy induced by biaxial strain and the Zeeman energy under magnetic field:

$$\mathcal{H}_{\text{Cr}} = D_0 S_z^2 + g_{\text{Cr}} \mu_B \vec{B} \cdot \vec{S}. \quad (\text{A1})$$

The exciton-Cr Hamiltonian can be separated into four parts

$$\mathcal{H}_{X-\text{Cr}} = \mathcal{H}_{\text{Cr}} + \mathcal{H}_{e-h} + \mathcal{H}_{\text{mag}} + \mathcal{H}_{c-\text{Cr}}, \quad (\text{A2})$$

where \mathcal{H}_{Cr} stands for the Cr alone. The electron-hole exchange interaction, \mathcal{H}_{e-h} , contains the short range and the long range parts. The short range contribution is a contact interaction which induces a splitting δ_0^{sr} of the bright and dark excitons and, in the reduced symmetry of a zinc-blend crystal (T_d), a possible coupling δ_2^{sr} of the two dark excitons. The long range part also contributes to the bright-dark splitting by an energy δ_0^{lr} . In QDs with C_{2v} symmetry (ellipsoidal flat lenses for instance [24]) the long range part also induce a coupling δ_1 between the bright excitons.

Realistic self-assembled QDs have symmetries which can deviate quite substantially from the idealized shapes of circular or ellipsoidal lenses. For a C_s symmetry (truncated ellipsoidal lens), additional terms coupling the dark and the bright excitons have to be included in the electron-hole exchange Hamiltonian. Following Ref. [24], the general form of the electron-hole exchange Hamiltonian in the heavy-hole exciton basis $|\uparrow_h \downarrow_e\rangle$, $|\downarrow_h \uparrow_e\rangle$, $|\uparrow_h \uparrow_e\rangle$, $|\downarrow_h \downarrow_e\rangle$ for a low symmetry QD (C_s) and for bright excitons linearly polarized along the (110) axis is

$$\mathcal{H}_{e-h} = \frac{1}{2} \begin{pmatrix} -\delta_0 & e^{i\pi/2} \delta_1 & e^{i\pi/4} \delta_{11} & -e^{i\pi/4} \delta_{12} \\ e^{-i\pi/2} \delta_1 & -\delta_0 & e^{-i\pi/4} \delta_{12} & -e^{-i\pi/4} \delta_{11} \\ e^{-i\pi/4} \delta_{11} & e^{i\pi/4} \delta_{12} & \delta_0 & \delta_2 \\ -e^{-i\pi/4} \delta_{12} & -e^{i\pi/4} \delta_{11} & \delta_2 & \delta_0 \end{pmatrix}. \quad (\text{A3})$$

An external magnetic field couples via the standard Zeeman terms to the carriers spins and a diamagnetic shift of the electron-hole pair is also included resulting in

$$\mathcal{H}_{\text{mag}} = g_e \mu_B \vec{B} \cdot \vec{\sigma} + g_h \mu_B \vec{B} \cdot \vec{J} + \gamma B^2, \quad (\text{A4})$$

where $\vec{\sigma}$ and \vec{J} stand for the angular momentum operator of the electron and hole, respectively.

$\mathcal{H}_{c-\text{Cr}}$ describes the coupling of the electron and hole spins with the Cr spin. It reads

$$\mathcal{H}_{c-\text{Cr}} = I_{e\text{Cr}} \vec{S} \cdot \vec{\sigma} + I_{h\text{Cr}} \vec{S} \cdot \vec{J} \quad (\text{A5})$$

with $I_{e\text{Cr}}$ and $I_{h\text{Cr}}$ the exchange integrals of the electron and hole spins with the Cr spin \vec{S} .

To limit the size of the density matrix and then the computing time in the calculation of the populations of the different spin states in Cr doped QDs we do not take into account the full valence band but only consider the heavy-hole subspace (\uparrow_h , \downarrow_h) and take into account a possible valence band mixing light holes (\uparrow_h , \downarrow_h) induced by an in-plane anisotropy through a pseudospin formalism. In the limit of weak valence band mixing the ground states of the holes in self-assembled QDs

can be written:

$$\begin{aligned} |\tilde{\uparrow}\rangle &\propto |\uparrow_h\rangle - \frac{\rho_{vbm}}{\Delta_{lh}} e^{2i\theta} |\downarrow_h\rangle \\ |\tilde{\downarrow}\rangle &\propto |\downarrow_h\rangle - \frac{\rho_{vbm}}{\Delta_{lh}} e^{-2i\theta} |\uparrow_h\rangle, \end{aligned} \quad (\text{A6})$$

where ρ_{vbm} is the mixing energy between heavy holes and light holes separated in energy by Δ_{lh} . A development of the hole

TABLE I. Values of the carrier-carrier and carrier-Cr exchange parameters used in the spin dynamics model presented in Fig. 7 and in the PL intensity map presented in Fig. 9. The value of the parameters not listed in the table is 0.

$I_{e\text{Cr}}$ μeV	$I_{h\text{Cr}}$ μeV	δ_0 meV	δ_1 μeV	δ_{12} μeV	δ_{11} μeV
	220				50
-30	D_0	-800	200	200	γ
$\frac{\rho_{vbm}}{\Delta_{lh}}$	meV	g_{Cr}	g_e	g_h	$\mu\text{eV}/T^2$
0.08	2.2	2	-1	0.4	1.25

TABLE II. Material (CdTe) [49] and QD parameters used in the calculation of the coupled hole and Cr spin relaxation time presented in Fig. 6.

CdTe		
Deformation potential constants	$ b $	1.0 eV
	$ d $	4.4 eV
Longitudinal sound speed	c_l	3300 m/s
Transverse sound speed	c_t	1800 m/s
Density	ρ	5860 kg/m ³
Quantum dot		
Cr-hole exchange energy	I_{hCr}	0.22 meV
hh-lh exciton splitting	Δ_{lh}	25 or 50 meV
Hole wave function widths:		
-in-plane	l_{\perp}	3.0 nm
-z-direction	l_z	1.25 nm

angular momentum operator \vec{J} in this subspace gives in the first order of $\frac{\rho_{vbm}}{\Delta_{lh}}$:

$$\tilde{J}_+ = \frac{\rho_{vbm}}{\Delta_{lh}} \begin{pmatrix} 0 & -2\sqrt{3}e^{-2i\theta_s} \\ 0 & 0 \end{pmatrix} \quad (A7)$$

$$\tilde{J}_- = \frac{\rho_{vbm}}{\Delta_{lh}} \begin{pmatrix} 0 & 0 \\ -2\sqrt{3}e^{2i\theta_s} & 0 \end{pmatrix} \quad (A8)$$

$$\tilde{J}_z = \begin{pmatrix} 3/2 & 0 \\ 0 & -3/2 \end{pmatrix} \quad (A9)$$

the pseudospin ladder operator \tilde{J}_+ and \tilde{J}_- flip the hole spin whereas the z component \tilde{J}_z confirms that these states are mainly heavy holes. This pseudospin description of the hole ground states is sufficient to describe the main consequences of valence band mixing in most of the self-assembled QDs.

In this simplified model we also neglect, within the biexciton, the interaction of spin paired carriers with the magnetic atom and the spin effective Hamiltonian of X_2 -Cr is given by

$$H_{X_2-Cr} = H_{Cr} + 2\gamma B^2. \quad (A10)$$

Table I present the list of parameters used to calculate the PL intensity map of an exciton in a Cr doped QD presented

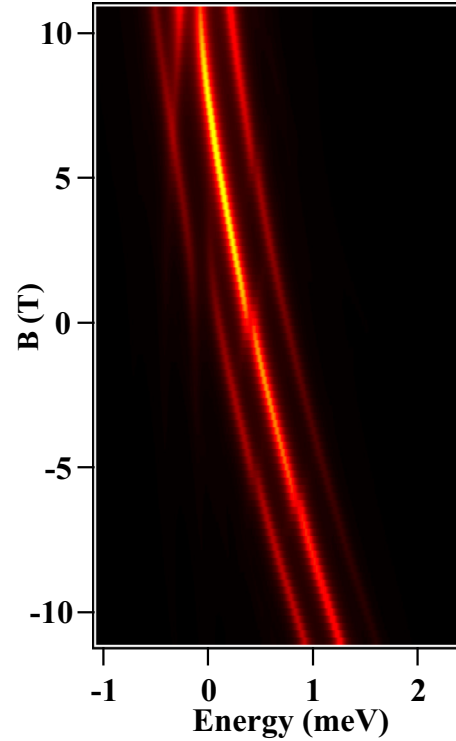


FIG. 9. (a) Intensity map of the magnetic field dependence of the σ -PL spectra of a Cr-doped QD calculated with the parameters listed in Table I. A thermalization on the exciton-Cr levels with $T_{\text{eff}} = 40$ K is used for a simplified description of the PL intensity distribution.

in Fig. 9. These parameters correctly reproduce the observed magnetic field dependence of QD1. They are used, together with the parameters of Table II, in the model of the spin dynamics presented in Fig. 7. However, let us notice that some of the parameters cannot be precisely determined or determined independently. For instance the splitting of the central line arises both from the long range part of the electron-hole exchange interaction and the short range part in the presence of valence band mixing. The two contributions cannot be separated and for a general description we use non null value for both of them. As the parameters listed in Table I give good orders of magnitude for the PL lines splittings, they are expected to also qualitatively describe the dynamics of coupled carriers and Cr spins.

[1] M. Veldhorst, C. H. Yang, J. C. C. Hwang, W. Huang, J. P. Dehollain, J. T. Muhonen, S. Simmons, A. Laucht, F. E. Hudson, K. M. Itoh, A. Morello, and A. S. Dzurak, *Nature (London)* **526**, 410 (2015).
 [2] S. Schmitt, T. Gefen, F. M. Stürmer, T. Unden, G. Wolff, C. Müller, J. Scheuer, B. Naydenov, M. Markham, S. Pezzagna, J. Meijer, I. Schwarz, M. Plenio, A. Retzker, L. P. McGuinness, and F. Jelezko, *Science* **356**, 832 (2017).
 [3] L. Besombes, Y. Leger, L. Maingault, D. Ferrand, H. Mariette, and J. Cibert, *Phys. Rev. Lett.* **93**, 207403 (2004).
 [4] M. Goryca, T. Kazimierzczuk, M. Nawrocki, A. Golnik, J. A. Gaj, P. Kossacki, P. Wojnar, and G. Karczewski, *Phys. Rev. Lett.* **103**, 087401 (2009).

[5] C. Le Gall, R. S. Kolodka, C. Cao, H. Boukari, H. Mariette, J. Fernandez-Rossier, and L. Besombes, *Phys. Rev. B* **81**, 245315 (2010).
 [6] C. Le Gall, A. Brunetti, H. Boukari, and L. Besombes, *Phys. Rev. Lett.* **107**, 057401 (2011).
 [7] L. Besombes, C. L. Cao, S. Jamet, H. Boukari, and J. Fernandez-Rossier, *Phys. Rev. B* **86**, 165306 (2012).
 [8] A. Kudelski, A. Lemaitre, A. Miard, P. Voisin, T. C. M. Graham, R. J. Warburton, and O. Krebs, *Phys. Rev. Lett.* **99**, 247209 (2007).
 [9] O. Krebs and A. Lemaitre, *Phys. Rev. Lett.* **111**, 187401 (2013).
 [10] A. O. Govorov and A. V. Kalameitsev, *Phys. Rev. B* **71**, 035338 (2005).

- [11] D. E. Reiter, V. M. Axt, and T. Kuhn, *Phys. Rev. B* **87**, 115430 (2013).
- [12] J. Kobak, T. Smolenski, M. Goryca, M. Papaj, K. Gietka, A. Bogucki, M. Koperski, J.-G. Rousset, J. Suffczynski, E. Janik, M. Nawrocki, A. Golnik, P. Kossacki, and W. Pacuski, *Nat. Commun.* **5**, 3191 (2014).
- [13] T. Smolenski, T. Kazimierczuk, J. Kobak, M. Goryca, A. Golnik, P. Kossacki, and W. Pacuski, *Nat. Commun.* **7**, 10484 (2016).
- [14] A. Lafuente-Sampietro, H. Utsumi, H. Boukari, S. Kuroda, and L. Besombes, *Phys. Rev. B* **93**, 161301(R) (2016).
- [15] J. T. Vallin and G. D. Watkins, *Phys. Rev. B* **9**, 2051 (1974).
- [16] J. Teissier, A. Barfuss, P. Appel, E. Neu, and P. Maletinsky, *Phys. Rev. Lett.* **113**, 020503 (2014).
- [17] A. Lafuente-Sampietro, H. Boukari, and L. Besombes, *Phys. Rev. B* **92**, 081305(R) (2015).
- [18] D. Lee, K. W. Lee, J. V. Cady, P. Ovarthaiyapong, and A. C. Bleszynski Jayich, *J. Opt.* **19**, 033001 (2017).
- [19] P. Rabl, S. J. Kolkowitz, F. H. L. Koppens, J. G. E. Harris, P. Zoller, and M. D. Lukin, *Nat. Phys.* **6**, 602 (2010).
- [20] P. Ovarthaiyapong, K. W. Lee, B. A. Myers, and A. C. Bleszynski Jayich, *Nat. Commun.* **5**, 4429 (2014).
- [21] A. Lafuente-Sampietro, H. Utsumi, H. Boukari, S. Kuroda, and L. Besombes, *Phys. Rev. B* **95**, 035303 (2017).
- [22] M. K. Kneip, D. R. Yakovlev, M. Bayer, A. A. Maksimov, I. I. Tartakovskii, D. Keller, W. Ossau, L. W. Molenkamp, and A. Waag, *Phys. Rev. B* **73**, 035306 (2006).
- [23] P. Wojnar, C. Bougerol, E. Bellet-Amalric, L. Besombes, H. Mariette, and H. Boukari, *J. Crystal Growth* **335**, 28 (2011).
- [24] M. Zielinski, Y. Don, and D. Gershoni, *Phys. Rev. B* **91**, 085403 (2015).
- [25] C. Le Gall, L. Besombes, H. Boukari, R. Kolodka, J. Cibert, and H. Mariette, *Phys. Rev. Lett.* **102**, 127402 (2009).
- [26] L. Besombes, K. Kheng, L. Marsal, and H. Mariette, *Phys. Rev. B* **63**, 155307 (2001).
- [27] L. Besombes, Y. Leger, L. Maingault, D. Ferrand, H. Mariette, and J. Cibert, *Phys. Rev. B* **71**, 161307(R) (2005).
- [28] P. Kacman, *Semicond. Sci. Technol.* **16**, R25 (2001).
- [29] J. Kossut and W. Dobrowolski, *Handbook of Magnetic Materials*, Vol. 7, Chap. 4, edited by K. H. J. Buschow (Elsevier Science Publisher, Amsterdam, 1993).
- [30] J. Blinowski and P. Kacman, *Phys. Rev. B* **46**, 12298 (1992).
- [31] M. Brousseau, *Les Defauts Ponctuels Dans Les Semiconducteurs* (Les Editions de Physique, Les Ulis, 1988).
- [32] J. Blinowski, P. Kacman, and J. A. Majewsky, *J. Crystal Growth* **159**, 972 (1996).
- [33] S. Kuroda, N. Nishizawa, K. Takita, M. Mitome, Y. Bando, K. Osuch, and T. Dietl, *Nat. Mater.* **6**, 440 (2007).
- [34] A. Continenza and S. Massidda, *Phys. Rev. B* **50**, 11949 (1994).
- [35] E. Rzepka, Y. Marfaing, M. Cuniot, and R. Triboulet, *Mater. Sci. Eng.* **B16**, 262 (1993).
- [36] A. Lafuente-Sampietro, H. Boukari, and L. Besombes, *Phys. Rev. B* **95**, 245308 (2017).
- [37] C. L. Cao, L. Besombes, and J. Fernandez-Rossier, *Phys. Rev. B* **84**, 205305 (2011).
- [38] E. Tsitsishvili, R. V. Baltz, and H. Kalt, *Phys. Rev. B* **67**, 205330 (2003).
- [39] K. Roszak, V. M. Axt, T. Kuhn, and P. Machnikowski, *Phys. Rev. B* **76**, 195324 (2007).
- [40] L. C. Lew, Y. Voon, and M. Willatzen, *The k.p Method* (Springer, Berlin, 2009).
- [41] P. Michler, *Single Quantum Dots Fundamentals, Applications and New Concepts* (Springer, Berlin, 2003).
- [42] J.-W. Luo, G. Bester, and A. Zunger, *Phys. Rev. B* **92**, 165301 (2015).
- [43] M. P. van Exter, J. Gudat, G. Nienhuis, and D. Bouwmeester, *Phys. Rev. A* **80**, 023812 (2009).
- [44] C. Roy and S. Hughes, *Phys. Rev. X* **1**, 021009 (2011).
- [45] S. Haroche and J.-M. Raimond, *Exploring the Quantum* (Oxford University Press, New York, 2006).
- [46] S. Jamet, H. Boukari, and L. Besombes, *Phys. Rev. B* **87**, 245306 (2013).
- [47] A. Hundt, J. Puls, A. V. Akimov, Y. H. Fan, and F. Henneberger, *Phys. Rev. B* **72**, 033304 (2005).
- [48] M. J. A. Schuetz, E. M. Kessler, G. Giedke, L. M. K. Vandersypen, M. D. Lukin, and J. I. Cirac, *Phys. Rev. X* **5**, 031031 (2015).
- [49] S. Adachi, *Properties of Group IV, III-V and II-VI Semiconductors* (John Wiley and Sons Ltd, Chichester, 2005).